



North Pacific Fisheries Commission

NPFC-2024-SSC PS14-IP03 (Rev. 1)

Spatio-temporal variability of density distribution of Pacific saury (*Cololabis saira*) and its relationship to basin-scale Ocean environmental variability in the North Pacific

Jihwan Kim^{1*}, Christopher N. Rooper¹, Libin Dai¹, Shin-Ichiro Nakayama¹, Miyako Naya¹, Hyejin Song¹, Yi-Jay Chang¹, Jhen Hsu¹, Vladimir Kulik¹, Rocky KaKu¹, Robert Day¹, Aleksandr Zavolokin¹, Rentaro Mitsuyu¹, and Toshihide Kitakado¹

¹North Pacific Fisheries Commission, Tokyo, Japan

*Corresponding author: Jihwan Kim (tho3ov@gmail.com)

North Pacific Fisheries Commission, Tokyo 108-8477, Japan

Keywords: CPUE, Kuroshio Extension Jet, North Pacific Gyre Oscillation, Pacific saury

Abstract

This study is the first to perform integration and spatio-temporal decomposition of gridded data from all members of the North Pacific Fisheries Commission to analyze variability in nominal catch per unit effort (CPUE) of Pacific saury (*Cololabis saira*), a species of significant socio-economic importance in the Northwestern Pacific. The results reveal three leading CPUE modes linked to basin-scale environmental factors: subsurface temperature in the Oyashio Current region, Kuroshio Extension dynamics, and biological productivity in the Kuroshio-Oyashio Extension region. These modes reflect long-term trends and shifts in density distribution of Pacific saury across the Northwestern Pacific. The first mode reveals a distinct seasonal fishing pattern, while the second and third modes indicate zonal and meridional distribution shifts, respectively. The results also suggest a correlation between CPUE variability and the North Pacific Gyre Oscillation, implying a connection to basin-scale ocean environmental variability. The results are valuable for refining Pacific saury stock assessments and understanding the wider marine ecosystem's relationship to ocean environmental change.

1. Introduction

The Pacific saury (*Cololabis saira*) is a commercially important species for several members of the North Pacific Fisheries Commission (NPFC) (Huang, 2010; Miyamoto et al., 2020; NPFC, 2021). Its widespread distribution throughout the mid-latitude North Pacific reflects its adaptability to a variety of ocean habitats and its robust migratory capabilities (Fukushima, 1979; Huang, 2010; Huang & Huang, 2015; Hubbs, 1980; NPFC, 2023c).

The Pacific saury has a distinct reproductive and migratory cycle that begins with the main winter spawning along the coast of Japan (Fuji, Kurita, Suyama, & Ambe, 2021; Iwahashi, Isoda, ITO, Oozeki, & Suyama, 2006; Kosaka, 2000; Suyama, 2002; K. Watanabe, Tanaka, Yamada, & Kitakado, 2006). Following spawning, the early life stages are transported eastward via the Kuroshio Extension current into the open ocean and the Transition Zone of the Northwestern Pacific, typically during June and July (Hashimoto et al., 2020; Miyamoto et al., 2020). Subsequently, the juvenile saury migrates northward into the NPFC Convention Area, where they feed on abundant zooplankton (Y. Watanabe, Kurita, Noto, Oozeki, & Kitagawa, 2003; Y. Watanabe & Lo, 1993). As they mature, Pacific saury undertake a westward migration, returning to their spawning grounds at one to two years of age, a journey that is highly influenced by prevailing ocean conditions (Kosaka, 2000; Suyama, 2002). Given the complex interplay between the life history of Pacific saury and oceanographic processes, therefore, clarifying the potential relationships between their spatio-temporal distribution and environmental variability is crucial to improve the understanding of their migration dynamics and population structure.

However, the short life of the Pacific saury span of one to two years poses a challenge for sustainable fisheries management and conservation due to rapid population turnover. Pacific saury stock is managed internationally by the NPFC, the primary fishing season for Pacific saury extends from August to December, primarily within the National

Waters of Japan and Russia and the northwestern part of the NPFC Convention Area (NPFC, 2022). Fishing activity typically begins near the Kuril Islands in the northern region of the Northwestern Pacific and moves southwest (counter-clockwise) to follow the migration of saury to coastal waters near the National Waters of Japan (Huang, 2010; Huang & Huang, 2015).

The density distribution of Pacific saury may be influenced by a number of factors, including sea surface temperature (SST, shown in Figure 1a) and sea surface height (SSH, shown in Figure 1b) near the Kuroshio, thermocline depth within the Kuroshio-Oyashio Extension (KOE; 35–44° N, 141–175° E), and biological factors such as sea surface chlorophyll, zooplankton abundance, and net primary production (NPP), would affect the food resource of Pacific saury (Agency, 2023; Ichii et al., 2018; Liu et al., 2022; Yatsu & Watanabe, 2017). These diverse environmental and biological factors collectively contribute to the complex patterns observed in the density distribution of Pacific saury, underscoring the need for comprehensive studies to understand their interactions fully. The dynamics of these environmental variables are controlled by the interaction of the warm Kuroshio and cold Oyashio currents (Humston, Ault, Lutcavage, & Olson, 2000; ITO et al., 2004; Miller & Schneider, 2000). The southward intrusion of Oyashio current and the intensification of the Kuroshio current, along with the Kuroshio Extension Jet, enhance biological productivity in the KOE (Oozeki, Watanabe, & Kitagawa, 2004; Tian, Akamine, & Suda, 2003; Tseng et al., 2013). This increased productivity when these currents converge significantly influences the migration and feeding patterns of Pacific saury, affecting their populations and distributions not only within the National Waters of Japan and Russia but also throughout the main fishing region in the Convention Area (Agency, 2023; Ichii et al., 2018; Yatsu & Watanabe, 2017).

Figures 1c–d display the mean and 2-year low-pass filtered (10 months) standard deviation of Pacific saury catch per unit effort (CPUE) from 2007 to 2022, illustrating

interannual variability. This nominal CPUE is calculated as total catch divided by total operational days per 1-degree grid where the data comes from NPFC Members, the nomenclature for Members is taken from the NPFC membership list (China, Japan, Korea, Chinese Taipei, and Russia). The mean CPUE peaks in the National Waters of Japan, particularly east of Honshu and south of Hokkaido. High CPUE values are also observed in the northwestern part of the Convention area, particularly far east of Hokkaido. The interannual variability of CPUE shows a similar spatial pattern. Notably, there is greater variability along the east coast of Honshu and southeast of Hokkaido, which may reflect the timing of migratory patterns of Pacific saury schools during and after the fishing season as they move towards their spawning areas south of Japan (Huang, 2010; Huang & Huang, 2015; Miyamoto et al., 2020).

Figure 1e shows the standardized CPUE of each member of the NPFC. Before 2001, standardized CPUE data were only available from Japan and Russia, with additional data contributions from Korea and Chinese Taipei beginning after 2001. Standardized CPUE data from China have been included since 2013. The individual Members standardized CPUE has been generally declining since a peak in 2008, however, individual NPFC Members standardized CPUE are not consistent prior to 2017. The stock assessment of Pacific saury indicates that the biomass of Pacific saury has generally been declining since a peak in 2002 (NPFC, 2021, 2023a, 2023e). Between 2007 and 2022, there has been a marked shift in the distribution of Pacific saury catches from predominantly inside National Waters (approximately 80%) of Japan and Russia to the Convention Area (over 97%), highlighting a significant shift in fishing patterns and areas (NPFC, 2023a, 2023d). In recent years, there has been a marked decline in Pacific saury CPUE within the National Waters of Japan and Russia, a trend that extends to the broader Convention Area, has been of great concern (Figure 1e) (NPFC, 2021, 2022, 2023a, 2023d). This decline coincides with a decline in total

catch from a peak in around 2008 and an observed eastward shift in the central longitudinal zone of the Pacific saury density, potentially impacting catches within the National Waters of Japan and Russia, by intercepting fish as they migrate westward (Hashimoto et al., 2020; NPFC, 2023b, 2023d, 2023e).

Previous studies have found significant correlations between Pacific saury abundance and various climatic and oceanographic indices, such as the Southern Oscillation Index, the Pacific Decadal Oscillation Index, and sea surface temperatures in the Kuroshio region (Tian et al., 2003; Tian, Ueno, Suda, & Akamine, 2002; Tian, Ueno, Suda, & Akamine, 2004). They showed that El Niño events have positive effects on Pacific saury abundance with a one-year lag and that there may even be regime shifts in Pacific saury abundance corresponding to oceanic regime shifts in the Kuroshio region. However, these analyses were primarily based on data from specific regions within the Northwestern Pacific, rather than encompassing the entire distributional range of Pacific saury. This spatial limitation in data coverage may not fully represent Pacific saury population dynamics across its entire habitat. As a result, there remains a need for a more comprehensive analysis of Pacific saury CPUE variability across the broader Northwestern Pacific region.

Recent discussions, as detailed in NPFC (2023c), suggest that variations in CPUE and longitudinal shifts in Pacific saury density distribution may be linked to interannual to decadal changes in basin-scale ocean environmental conditions. These include potential effects of the North Pacific Gyre Oscillation (NPGO) and factors affecting Pacific saury recruitment or even distribution. The North Pacific Gyre Oscillation (NPGO) is suggested to influence Pacific saury abundance and CPUE by affecting the dynamics of the Kuroshio Extension Jet and biological productivity in the Kuroshio-Oyashio Extension (KOE) region, potentially with a 2-year delay (Ceballos, Di Lorenzo, Hoyos, Schneider, & Taguchi, 2009; Di Lorenzo et al., 2013; Di Lorenzo et al., 2008; NPFC, 2023c). However, the detailed

mechanistic pathways and statistical dynamics underlying these relationships have not been comprehensively defined or quantified.

Between 2007 and 2022, there has been a marked shift in the distribution of Pacific saury catches from predominantly inside National Waters (approximately 80%) of Japan and Russia to the Convention Area (over 97%), highlighting a significant shift in fishing patterns and areas (NPFC, 2023a, 2023d). This study examines the interannual variability of nominal CPUE of Pacific saury from 2007 to 2022 and investigates its spatio-temporal dynamics in the context of the basin-scale ocean environmental variability in the North Pacific to understand the long-term decline and eastward shift of CPUE in the Northwestern Pacific. This study operates under the assumption that CPUE variability correlates with the abundance of Pacific saury and that fishing vessels effectively track these saury schools, which respond dynamically to changes in the ocean environment. In this regard, observed spatial variability in fishing effort and spatial variability in CPUE primarily reflects the movement patterns of saury schools. While recognizing that factors such as fishing pressure and other anthropogenic effects also affect Pacific saury CPUE, this analysis focuses specifically on understanding the relationship between CPUE variability and broader ocean environmental variability.

2. Data and Method

2. 1. Fisheries Data

This study analyzed Pacific saury (*Cololabis saira*) catch and fishing effort data from 2007 to 2022, provided by member nations of the North Pacific Fisheries Commission (NPFC): China, Japan, Korea, Russia, Chinese Taipei, and Vanuatu. The catch per unit effort (CPUE) was calculated for each $1^\circ \times 1^\circ$ grid cell by dividing the total catch (in metric tons) by the total number of fishing days within that grid cell for each month. This nominal CPUE

serves as a proxy for Pacific saury density. The dataset encompasses the area 32–51°N and 140–174° E, covering the primary distribution range of Pacific saury in the Northwestern Pacific. Nominal CPUE represents the initial or unadjusted catch per unit effort, without adjusting for variables such as gear efficiency, fishing location, environmental conditions, or temporal shifts in the fish population.

2. 2. Ocean Environmental Variables

This study analyzed ocean environmental data from the North Pacific (0–60° N, 120° E–120° W) and mainly focused on the Northwestern Pacific (30–55° N, 130–175° E), the main fishing ground for Pacific saury, to examine the basin-scale ocean environmental variability and its impact on CPUE in the Northwestern Pacific. A range of Ocean environment datasets was obtained to analyze the physical and biological aspects of the North Pacific Ocean from 2007 to 2022. Monthly mean temperature, current velocity data to 300 m depth, and the SSH were obtained from Simple Ocean Data Assimilation (SODA) 3.15.2 at 0.5° spatial resolution (Carton & Giese, 2008). The SST data were obtained from the National Oceanic and Atmospheric Administration (NOAA) Optimum Interpolation SST v2.1 with a finer resolution of 0.25° (Reynolds, Rayner, Smith, Stokes, & Wang, 2002). In addition, monthly net primary production (NPP) data to depths of 300 m, which are critical for assessing biological productivity, were obtained from the Global Ocean Biogeochemistry Hindcast of the Copernicus Marine Environment Monitoring System Service at a resolution of 0.25° (*Global Ocean Biogeochemistry Hindcast*). The modeled chlorophyll fields in this dataset show a good agreement with satellite observations, which are widely regarded for their extensive spatial and temporal coverage. Satellite data effectively capture the dynamics of primary production, which is essential for understanding large-scale ecological structures and seasonal cycles. Although NPP data have inherent uncertainties, their strong correlation

with reliable satellite-derived measurements provides valuable insights into primary production patterns, underscoring the importance of the NPP dataset for studying biological productivity across ocean regions.

To investigate the relationship between the basin-scale ocean variability and CPUE of the Pacific saury, the North Pacific Gyre Oscillation (NPGO) index was analyzed from August to December each year using a 2-year low-pass filter to understand their interannual variability. All climate indices used in this study were obtained from NOAA (https://www.psl.noaa.gov/gcos_wgsp/Timeseries/).

2. 3. Cyclostationary Empirical Orthogonal Function (CSEOF)

The Pacific saury CPUE data exhibit highly periodic variability. To accurately capture and characterize these periodic spatial variations in the environmental data, this study employed Cyclostationary Empirical Orthogonal Function (CSEOF) analysis (Kwang-Yul Kim & North, 1997; Kwang-Yul Kim, North, & Huang, 1996). This method allows for the analysis and decompose of the spatio-temporal variability of ocean environmental variables, including SST, SSH, temperature and current velocity in the upper 300 meters, NPP, and the CPUE of Pacific saury. This method, widely used in numerous studies, is effective in examining specific time series and the physical-biological variability of environmental variables, particularly in the context of basin-scale ocean dynamics (J. Kim & Na, 2022; J. Kim, Na, Park, & Kim, 2020; Kwang-Yul Kim, Hamlington, & Na, 2015).

The target variables, including the ocean environmental variables at each depth, and the CPUE of the Pacific saury, $E(r, t)$, are decomposed into cyclostationary loading vectors (CSLVs), $B_n(r, t)$ and their corresponding principal component (PC) time series, $T_n(t)$ as in Eq. (1):

$$E(r, t) = \sum_n B_n(r, t)T_n(t), \quad (1)$$

where n , r , and t denote the number of modes, 2-dimensional space, and time, respectively. By convolving the zonal and meridional components, the current velocity was analyzed as a single variable. The CSLVs were derived to illustrate the physical evolution of environmental variables over a nested 5-month period (one fishing year; August to December). The n th mode of the CSLVs has periodicity d , as in Eq. (2):

$$B_n(r, t) = B_n(r, t + d) \quad (2)$$

Thus, $B_n(r, t)$ consists of 5 monthly spatial patterns (from August to December) which represent the physical evolution of the n th mode. Its corresponding PC time series, $T_n(t)$, illustrates the temporal variation (amplitude) of the n th mode. Each CSLV is orthogonal to the others. Figure 2–4 will later present the CSLVs and their corresponding PC time series for the three leading modes of the Pacific saury CPUE anomaly, with the total mean removed. The CSLVs for each mode will demonstrate the monthly spatio-temporal evolution of CPUE from August to December, effectively capturing both the spatial patterns and their temporal dynamics.

In the Northwestern Pacific, Pacific saury fishing vessels exhibit considerable size variation. While most international vessels exceed 400 gross registered tons (grt), Japanese vessels predominantly fall within the 19–199 grt range, classifiable as smaller vessels (designated as JP2). This study examines the influence of fleet composition on the variability of CPUE across modes by analyzing the effect of vessel size on the observed patterns, achieved by selectively omitting JP1 and JP2 data from the integrated dataset. Japanese

CPUE data were stratified into two categories based on vessel size: JP1, representing larger vessels (≥ 100 grt) and JP2, representing smaller vessels (< 100 grt). Analyses of the three dominant CPUE modes were conducted both including and excluding JP1 and JP2 data to assess the impact of fleet composition on CPUE patterns.

2. 4. Regression Analysis

This study investigated the statistical relationship between each CSEOF mode of the CPUE of Pacific saury in the Northwestern Pacific, denoted as $T_n(t)$ and $B_n(r, t)$, and ocean environmental variability through a regression analysis within the CSEOF space, as described in Eq. (3):

$$T_n(t) \approx \sum_{m=1}^N \alpha_m^{(n)} P_m(t), \quad (3)$$

where n represents the mode number for the CPUE, m the mode number for ocean environmental variable, $P_m(t)$ the PC time series of each ocean variable, and $\alpha_m^{(n)}$ is the regression coefficient between $T_n(t)$ and $P_m(t)$. Utilizing the regression coefficient $\alpha_m^{(n)}$, the regressed and reconstructed ocean environmental variability $R_n(r, t)$ can be derived as shown in Eq (4):

$$R_n(r, t) = \sum_{m=1}^N \alpha_m^{(n)} C_m(r, t), \quad (4)$$

where $C_m(r, t)$ represents the CSLVs of the ocean environmental variables. The evolution patterns in the ocean environment, denoted as $R_n(r, t)$, mirrors the variability $B_n(r, t)$ in the fishery data with the same PC time series $T_n(t)$ (Kwang-Yul Kim et al., 2015). As a

result, the regressed environmental patterns $R_n(r, t)$ reflect the environmental conditions associated with $B_n(r, t)$, and represent the prevalent conditions observed during periods of heightened amplitude in the PC time series $T_n(t)$ of the CPUE mode. In this study, a specific number of PC time series, designated as N , was selected for each regression based on the cumulative percentage of variance explained by the modes, typically ranging between 80–90%. Employing a limited number of components is advantageous as it reduces the risk of overfitting and enhances the stability of the predictions. The explanatory power of ocean environmental variables is indicated by R-squared values, annotated in each figure.

This study addressed potential autocorrelation in the residuals during the regression analysis by employing statistical methods to adjust the degrees of freedom (DOF), utilizing the Durbin-Watson statistic (Durbin & Watson, 1971; Kabaila, Farchione, Alhelli, & Bragg, 2021; White, 1992) to detect autocorrelation and the Cochrane-Orcutt procedure (Cochrane & Orcutt, 1949) to correct standard errors. These adjustments refined DOF estimates, enhancing the robustness of statistical tests. Significance testing was conducted using the F statistics, with a critical p value threshold set at less than 0.01 to achieve a confidence level exceeding 99%.

Despite the inherent smoothing effects of the CSEOF principal component time series (Kwang-Yul Kim & North, 1997; Kwang-Yul Kim et al., 1996), the consistently low p values (< 0.001) of all regressions affirm the high statistical significance of the findings. The residual DOF for each regression analysis, adjusted for autocorrelation using the Durbin-Watson statistic and the Cochrane-Orcutt procedure, are detailed in Supplementary Table 1. The corresponding F statistics and low p values demonstrate that variations in CPUE are largely explained by ocean environmental variables.

While fishing pressure and other anthropogenic factors may also influence CPUE, the analysis suggests that environmental factors play a significant role. This does not negate

the potential impacts of fishing pressure and anthropogenic factors, but highlights the substantial explanatory power of environmental variables within the analyzed CPUE variability. However, it is important to clarify that this statistical correlation does not imply causality between ocean environmental variability and CPUE variability. Rather, it indicates a significant association between them that warrants further investigation of their dynamic interplay.

2. 5. Composite Analysis

A composite analysis was conducted, examining Pacific saury CPUE variability related to the 2-year low-pass filtered NPGO index during its positive and negative phases exceeding or falling below one standard deviation. To assess statistical significance, this study used two-sample t-tests that account for autocorrelation and adjust for effective degrees of freedom to compare mean CPUE values in each grid cell between the positive and negative NPGO phases.

3. Results

3. 1. Three dominant modes of variability in CPUE

Figure 2 illustrates the first three modes of Cyclostationary loading vectors and their corresponding PC time series for Pacific saury CPUE anomaly, with the total mean removed, in the Northwestern Pacific, spanning August to December (refer to the method section). These modes, each account for approximately 10% or more of the total variance, collectively represent over half of the CPUE variability.

The first mode of CPUE (left column in Figure 2), which accounts for approximately 30% of the total variance, shows a remarkable temporal and spatial evolution of the loading vectors. During the positive phase of the corresponding PC time series, beginning in August,

an increase of the CPUE emerges south of the Kuril Islands, extending and shifting westward to the south of Hokkaido, east of Honshu, and the coastline by October. This increase reaches its peak south of Hokkaido and east of Honshu and persists through November, then diminishes and retreats southward. Concurrently, decreases in the CPUE are observed east of Honshu, south of Hokkaido, and in the Northwestern part of the Convention Area. This pattern is consistent with the typical fishing season of August through December and with the known migratory pattern (dynamic fishing grounds from North to South) of Pacific saury returning to the coast of Japan to spawn. The corresponding PC time series shows predominantly positive values until 2019 and periodicity of 3–5 fishing years. Since 2019, the PC time series has been negative, with an overall long-term decreasing trend suggesting a decrease in the Pacific saury CPUE over the past decade.

The second mode of CPUE (middle column in Figure 2), which accounts for approximately 15% of the total variance, reveals contrasting anomalies within and outside the Convention Area. During the positive phases of its corresponding PC time series, there is a general decrease in CPUE south of Hokkaido and east of Honshu, while an increase in CPUE is observed in the northwestern part of the Convention Area. The latter appears in September, intensifies in October, and then decays in December. The PC time series of this mode shows a long-term increasing trend with a periodicity of 3–4 fishing years, reflecting a notable shift in the dynamics of the Pacific saury fishery. Specifically, the CPUE of Pacific saury exhibits a decreasing trend in the south of Hokkaido and east of Honshu and an increasing trend in the Convention Area according to this mode. This may be indicative of a significant long-term zonal shift, characterized primarily by an eastward shift pattern from the National Waters of Japan to the Convention Area in the Northwestern Pacific over the past decade. The eastward shift is associated with smaller and more discontinuous positive anomalies in the Northwestern part of the Convention Area, suggesting a more dispersed and possibly patchy

density of Pacific saury.

During the positive phase of the corresponding PC time series, the third mode of CPUE (illustrated in the right column of Figure 2), which accounts for approximately 10% of the total variance, initially displays increases in CPUE south of the Kuril Islands from August to September. These increases manifest along the east coast of Honshu in October, expanding both northward and southward as they intensify through December, while south of the Kuril Islands from September to October. This mode reflects a meridional shift in CPUE variability, i.e. the latitudinal migration of CPUE increases along the east coast of Honshu. The PC time series for this mode exhibits a biennial fluctuation until 2019, without a clear long-term trend, reflecting a north-south migration pattern in the spatial and temporal distribution of Pacific saury CPUEs.

To investigate the potential influence of fleet composition on CPUE variability, this study examined the effect of vessel size on observed patterns across modes. Japanese CPUE data were stratified into two categories based on vessel size: JP1 (larger vessels) and JP2 (smaller vessel). Analyses of the first three dominant CPUE modes were conducted both with and without JP1 and JP2 data to assess the effect of fleet composition.

Excluding the JP1 data resulted in comparable spatio-temporal variability for the first two dominant modes (Figures 2 and 3). While minor deviations in the loading vectors of the third mode were observed along the east coast of Honshu, overall spatial coherence was maintained. Conversely, excluding the JP2 data resulted in spatio-temporal variability patterns that were largely consistent with the original CPUE data across all modes (Figures 2 and 4). In particular, the first CPUE mode showed pronounced positive anomalies along the east coast of Honshu during its positive phase.

These results suggest that fleet composition effects on Pacific saury CPUE are primarily localized to the east coast of Honshu, presumably due to operational characteristics

related to vessel size. The wider northwestern Pacific appears to be minimally affected. This suggests that the observed spatial patterns in CPUE are generally robust to vessel size effects.

3. 2. Ocean conditions associated with three dominant modes of CPUE variability

Figure 5 presents the annual average anomalies of ocean environmental variables that have been regressed and reconstructed for each CPUE mode, specifically during the positive phases of their respective time series. The R-squared values for each regression, shown in parentheses, indicate that these environmental variables account for a substantial portion of the variability in CPUE. For the first CPUE mode (left column), the SST anomaly generally reflects surface cooling, except for a warming trend in the eastern Equatorial Pacific (Figure 5a). The SSH anomaly (Figure 5d) shows a distinct dipole pattern east of Honshu, with a positive anomaly north of 35° N and a negative anomaly south, indicating a weakening of the Kuroshio Extension Jet, a trend also observed in the subsurface current anomalies (Figure 5g). The associated subsurface temperature anomaly (Figure 5g) shows widespread warming in the southern Sea of Okhotsk and cooling south of Hokkaido. The NPP anomalies show a generally positive trend at the surface, particularly in the south of Hokkaido and east of Honshu, south of the Kuril Islands, and the Convention Area (Figure 5j), with significant positive subsurface anomalies south of 35° N along the Kuroshio and its Extension Jet. In contrast, the NPP shows negative anomalies along the east coast of Honshu and in the Northwestern part of the Convention Area (Figure 5m).

For the second CPUE mode (middle column), Regressed and reconstructed SST anomaly pattern shows a widespread warming, particularly northwest of northwest of North America and in the Equatorial Pacific (Figure 5b). The SSH pattern (Figure 5e) shows a significant negative anomaly south of Honshu and a positive anomaly near the latitude of the Kuroshio Extension Jet (35° N), indicating the strengthening of the Jet. The subsurface

current anomalies (Figure 5h) east of Honshu also show physically consistent spatial patterns of Jet strengthening. The subsurface temperature anomaly contrasts with the first mode (Figures 5g–h), indicating an overall warming except in the southern Sea of Okhotsk. The NPP anomalies (Figures 5j–k and 5m–5n) show contrasting spatial patterns between the first and the second modes, with positive surface anomalies in the southern Sea of Okhotsk and the far eastern region (Figure 5k), and significantly negative subsurface anomalies south of the Kuroshio Extension Jet, but positive along the east coast of Honshu and in the Northwestern part of the Convention Area (Figure 5n).

Regressed onto the third CPUE mode (right column), SST anomalies (Figure 5c) predominantly indicate cooling, except for surface warming in the marginal seas around Korea and China, the Equatorial Pacific, and from 30° N to 50° N east of 160° E to 180°, which show surface warming. The SSH anomalies (Figures 5d and 5f) show a pattern similar to the first mode with a positive anomaly south of Honshu and north of the Kuroshio Extension Jet. The current anomaly also suggests a weakening of the Kuroshio Extension Jet, while the subsurface temperature (Figures 5g and 5i) shows general warming, especially in the southern Sea of Okhotsk. The NPP anomalies associated with this mode (Figures 5l and 5o) have less explanatory power at both the surface and subsurface depths compared to the first and the second mode. They exhibit negative surface variability south of 42.5° N and positive anomalies southeast of Hokkaido. Subsurface NPP show negative anomalies in the Kuroshio and south of its extension, but positive anomalies east of 150° N.

4. Discussion

4. 1. Ocean conditions during the high CPUE period

While the first mode of CPUE reflects the migratory patterns of Pacific saury, primarily around Honshu from September to November, concerns persist regarding the

mode's depiction of a decreasing trend in CPUE without adjusting for fishing pressure. This raises caution about attributing changes in this CPUE mode solely to ocean environmental variability, as the influence of fishing pressure could also be significant. However, the statistical significance tested in this study indicates that ocean environmental variables significantly and reasonably explain variations in this CPUE mode. While it is important to consider the potential impacts of fishing pressure, the results suggest that ocean environmental conditions play a substantial role in influencing this mode of CPUE. Further study incorporating both environmental and anthropogenic factors would provide a more comprehensive understanding of the influences on CPUE variability.

When regressed onto the first CPUE mode during the positive phase of its corresponding PC time series, the SST anomaly shows general cooling across the North Pacific, accompanied by noticeable warming in the eastern Equatorial Pacific. Concurrently, the SSH anomaly reveals a significant positive anomaly south of Japan and a predominant negative anomaly throughout the Kuroshio Extension (left column of Figure 5). The subsurface cooling along the east coast of Honshu and south of Hokkaido suggests an intensified Oyashio Current, which may enhance the flow of nutrient-rich water to the nearshore areas (Saito, Tsuda, & Kasai, 2002; Tseng et al., 2014; Yasuda & Watanabe, 1994). In addition, warming in the southern part of the Sea of Okhotsk may promote phytoplankton blooms, as indicated by the positive surface NPP anomaly around the Kuril Islands (S. T. Kim, 2012; Kishi et al., 2021; Mustapha & Saitoh, 2008). Positive NPP anomalies at the surface and around the Kuroshio and its Extension Jet in the subsurface suggest biologically favorable conditions for Pacific saury, potentially leading to increased CPUE near and off the east coast of Honshu (left column in Figure 2) (Ceballos et al., 2009; Chhak, Di Lorenzo, Schneider, & Cummins, 2009).

The regressed and reconstructed SST and SSH anomalies, onto the second mode of

CPUE (middle column in Figure 5), display spatial patterns similar to those observed at the peak of a positive NPGO year (Ceballos et al., 2009; Di Lorenzo et al., 2013; Di Lorenzo et al., 2008). This similarity may indicate a potential relationship between the second mode of the CPUE and the NPGO. The SSH and subsurface current anomalies in the second mode indicate a strengthened Kuroshio Extension Jet, suggesting an eastward intensified zonal current. The surface to subsurface NPP anomalies show increased biological productivity far east of Honshu and within the Convention Area. This increased eastward current velocity and increased biological productivity are likely to facilitate an eastward migration of Pacific saury, which may result in increased CPUE in the Convention Area and decreased CPUE near Japan (middle column in Figure 2).

Understanding the relationship between the third CPUE mode and both SST and subsurface temperature anomalies presents challenges (right column in Figure 5). However, the SSH pattern is characterized by a positive anomaly south of Honshu and north of the Kuroshio Extension Jet, with a notable divergence in the negative anomaly south of the Jet. Additionally, the subsurface current anomaly indicates a weakening of the Kuroshio Extension Jet. This weakening may facilitate the transport of phytoplankton toward the southern nearshore regions of Japan (Honshu) at subsurface depths, potentially explaining the increased CPUE observed along the southern east coast of Honshu in the third CPUE mode (right column in Figure 2).

4. 2. Basin-scale Ocean environmental variability and high CPUE

The spatial patterns of SST and SSH anomalies regressed onto the second mode of CPUE variability exhibit similarities to those associated with the NPGO. This correspondence in spatial patterns, as illustrated in the middle column of Figure 5, may suggest a potential relationship between CPUE variability and the NPGO. Additionally,

analysis of long-term historical data (1950–2020) reveals a significant correlation ($r = 0.51, p < 0.01$ with a 2-year lag) between Pacific saury catches within the Convention Area and the NPGO index. This correlation may suggest that the observed short-term relationships may reflect underlying ecological processes. However, interpreting this relationship faces challenges such as the varying quality of historical data over time, the limited temporal extent of the CPUE dataset, and the fact that the correlation is based on catches rather than CPUE. These issues potentially affect statistical reliability due to autocorrelation and reduced DOF. To address these limitations and more robustly explore the relationship between CPUE and basin-scale ocean environmental variability, this study employs composite analysis.

Figure 6 presents the results of a composite analysis, examining Pacific saury CPUE variability related to the 2-year low-pass filtered NPGO index during its positive and negative phases exceeding or falling below one standard deviation. During the positive phase of NPGO, CPUE exhibits positive anomalies east of Honshu and south and east of Hokkaido, contrasted by slight negative anomalies in the Northwestern part of the Convention Area. Conversely, the negative phase of the NPGO is characterized by reverse patterns, with negative anomalies around Honshu and Hokkaido and positive anomalies in the Convention Area. These patterns were statistically significant in the areas described, particularly in the regions east of Honshu, south of Hokkaido, and the Northwestern part of the Convention Area.

The spatial distribution of CPUE anomalies shows a consistent alignment with the patterns observed in the second mode of CPUE variability. This alignment suggests a longitudinal shift in CPUE distribution that correlates with NPGO phases that influence biological productivity in the KOE region (Ceballos et al., 2009; Di Lorenzo et al., 2013; Di Lorenzo et al., 2008) and, consequently, may induce a longitudinal shift in Pacific saury density. This observed correspondence between CPUE variability and NPGO phases

underscores the potential link of the NPGO to both the spatial distribution and magnitude of CPUE, and emphasizes the need to incorporate large-scale ocean environmental variability into our understanding of the spatio-temporal dynamics of the Pacific saury fishery.

While this result indicates a possible connection between the NPGO and CPUE variability, it is essential to recognize that the NPGO is not the sole influencing factor. Other climatic indices such as the Pacific Decadal Oscillation and El Niño-Southern Oscillation may also significantly impact CPUE variability, highlighting the need for further research into the complex dynamics that govern marine ecosystems and fishery productivity (Oozeki et al., 2004; Tseng et al., 2013). In addition, the mechanisms underlying the observed relationships between NPGO and CPUE patterns are not fully understood and may involve complex ecological and oceanographic processes.

5. Concluding remarks

The variability in Pacific saury CPUE over recent decades has been effectively extracted into three dominant modes, which collectively explain over half of the total variability in CPUE. These modes can be related in terms of physical environmental variability in the ocean and are critical in highlighting the recent CPUE patterns. In particular, the first two modes explain the overall decline in CPUE time series over the last decade and the eastward migration (the second mode of CPUE) associated with the reduction in the overall CPUE (the first mode of CPUE). Furthermore, the results show potential relationship between the CPUE and the NPGO, underscoring the profound influence of large-scale ocean conditions on the dynamics of Pacific saury CPUEs (Kuroda & Yokouchi, 2017; Megrey et al., 2007; Tian et al., 2004).

The behavior of small pelagic species such as Pacific saury highlights the challenges of using CPUE as a simple measure of stock abundance. Due to their schooling behavior and

the effects of fishing mortality, Pacific saury populations can maintain high catch rate even during declines, making it difficult to accurately assess their abundance. This study focuses on a period of declining CPUE in the face of sustained fishing, during which aggregation of saury, possibly influenced by favorable ocean conditions could increase fishery yields. The decline in CPUE observed after 2006, as shown in Figure 1, is likely due to both fishing pressure and environmental factors. The statistically significant CPUE modes indicate that this relationship may be linked to recruitment dynamics. This finding underscores the need for management and conservation strategies for Pacific saury that take into account both environmental variability and fishing impacts, aiming for a comprehensive approach that addresses the multiple factors influencing stock fluctuations.

The long-term stability of the observed relationships between climate index and Pacific saury CPUE is uncertain, especially in the context of potential climate change impacts. Factors such as El Niño events, marine heat waves, and rising ocean temperatures could significantly affect phytoplankton populations, a critical food source for Pacific saury. In addition, increasing fishing pressure is an important factor that needs to be continuously assessed to determine its impact relative to environmental variability. Pacific saury population dynamics are influenced by both natural and anthropogenic factors, including fishing pressure. To better understand and manage these dynamics, it is critical to integrate environmental variables into future stock assessments. This integration would help estimate recruitment effects in population analyses and improve the utility of CPUE data. Standardizing CPUE annually by stock level could provide clearer insights into how environmental and human factors interact, thereby improving the management and sustainability of this important fishery.

The interpretation of nominal CPUE variability in this study is grounded on the data and analyses utilized; however, it is crucial to emphasize that these results do not negate the

impact of human activities, such as overfishing. Overfishing, along with illegal, unreported, and unregulated (IUU) fishing, continues to be a significant challenge in the high seas, adversely affecting both conservation efforts and scientific research. Stock assessments for Pacific saury have identified overfishing as a dominant factor since 2008, with the annual fishing removals surpassing the number of fish produced each year (NPFC, 2023b, 2023e). Additionally, the stock assessment indicates that a significant portion of the catch is comprised of age-0 Pacific saury, complicating the accurate determination of their natural mortality rates. Therefore, ongoing monitoring of fishing activities and continued dedication to conservation and research are imperative. It is important to clarify that the interpretations presented in this study do not represent the official position or viewpoint of the NPFC.

This study is the first comprehensive spatio-temporal decomposition analysis of 1-degree gridded monthly nominal CPUE for Pacific saury derived from catch data and operational days, integrating data from NPFC members operating vessels actively targeting Pacific saury (China, Japan, Korea, Russia, Chinese Taipei, and Vanuatu). The results highlight the spatio-temporal variability of CPUE, the effect of fleet size on CPUE, and propose a potential link between Pacific saury CPUE variability and basin-scale ocean environmental factors. This study provides valuable insights into the recent declining trend in Pacific saury catches in recent years.

References

- Carton, J. A., & Giese, B. S. (2008). A reanalysis of ocean climate using Simple Ocean Data Assimilation (SODA). *Monthly Weather Review*, *136*(8), 2999–3017.
- Ceballos, L. I., Di Lorenzo, E., Hoyos, C. D., Schneider, N., & Taguchi, B. (2009). North Pacific Gyre Oscillation synchronizes climate fluctuations in the eastern and western boundary systems. *Journal Of Climate*, *22*(19), 5163–5174.
- Chhak, K. C., Di Lorenzo, E., Schneider, N., & Cummins, P. F. (2009). Forcing of low-frequency ocean variability in the northeast Pacific. *Journal Of Climate*, *22*(5), 1255–1276.
- Cochrane, D., & Orcutt, G. H. (1949). Application of least squares regression to relationships containing auto-correlated error terms. *Journal Of The American Statistical Association*, *44*(245), 32–61.
- Di Lorenzo, E., Combes, V., Keister, J. E., Strub, P. T., Thomas, A. C., Franks, P. J., . . . Bograd, S. J. (2013). Synthesis of Pacific Ocean climate and ecosystem dynamics. *Oceanography*, *26*(4), 68–81.
- Di Lorenzo, E., Schneider, N., Cobb, K. M., Franks, P., Chhak, K., Miller, A. J., . . . Curchitser, E. (2008). North Pacific Gyre Oscillation links ocean climate and ecosystem change. *Geophysical Research Letters*, *35*(8).
- Durbin, J., & Watson, G. S. (1971). Testing for serial correlation in least squares regression. III. *Biometrika*, *58*(1), 1–19.
- Fuji, T., Kurita, Y., Suyama, S., & Ambe, D. (2021). Estimating the spawning ground of Pacific saury *Cololabis saira* by using the distribution and geographical variation in maturation status of adult fish during the main spawning season. *Fisheries Oceanography*, *30*(4), 382–396.
- Fukushima, S. (1979). Synoptic analysis of migration and fishing conditions of Pacific saury

- in the northwest Pacific Ocean. *Tohoku Reg Fish Res Lab*, 41, 1–70.
- Global Ocean Biogeochemistry Hindcast. *E.U. Copernicus Marine Service Information*.
<https://doi.org/10.48670/moi-00019>. Retrieved Jan 10, 2024.
- Hashimoto, M., Kidokoro, H., Suyama, S., Fuji, T., Miyamoto, H., Naya, M., . . . Kitakado, T. (2020). Comparison of biomass estimates from multiple stratification approaches in a swept area method for Pacific saury *Cololabis saira* in the western North Pacific. *Fisheries Science*, 86, 445–456.
- Hsu, J., Chang, Y.-J., Kitakado, T., Kai, M., Li, B., Hashimoto, M., . . . Park, K. J. (2021). Evaluating the spatiotemporal dynamics of Pacific saury in the Northwestern Pacific Ocean by using a geostatistical modelling approach. *Fisheries Research*, 235, 105821.
- Huang, W.-B. (2010). Comparisons of monthly and geographical variations in abundance and size composition of Pacific saury between the high-seas and coastal fishing grounds in the northwestern Pacific. *Fisheries Science*, 76(1), 21–31.
- Huang, W.-B., & Huang, Y.-C. (2015). Maturity characteristics of pacific saury during fishing season in the Northwest Pacific. *Journal of Marine Science and Technology*, 23(5), 27.
- Hubbs, C. (1980). Revision of the sauries (Pisces, Scomberesocidae) with descriptions of two new genera and one new species. *Fish. Bull.*, 77, 521–566.
- Humston, R., Ault, J. S., Lutcavage, M., & Olson, D. B. (2000). Schooling and migration of large pelagic fishes relative to environmental cues. *Fisheries Oceanography*, 9(2), 136–146.
- Ichii, T., Nishikawa, H., Mahapatra, K., Okamura, H., Igarashi, H., Sakai, M., . . . Usui, N. (2018). Oceanographic factors affecting interannual recruitment variability of Pacific saury (*Cololabis saira*) in the central and western North Pacific.

Fisheries Oceanography, 27(5), 445–457.

ITO, S. I., Kishi, M. J., Kurita, Y., Oozeki, Y., Yamanaka, Y., Megrey, B. A., & Werner, F. E. (2004). Initial design for a fish bioenergetics model of Pacific saury coupled to a lower trophic ecosystem model. *Fisheries Oceanography*, 13, 111–124.

Iwahashi, M., Isoda, Y., ITO, S. I., Oozeki, Y., & Suyama, S. (2006). Estimation of seasonal spawning ground locations and ambient sea surface temperatures for eggs and larvae of Pacific saury (*Cololabis saira*) in the western North Pacific. *Fisheries Oceanography*, 15(2), 125–138.

Japan Fisheries Research and Education Agency. (2023). サンマの不漁要因解明について (調査・研究の進捗) 令和5年4月 [Investigating the Causes of Poor Pacific Saury Catches (Progress of Research and Studies) April 2023]. Retrieved Jan 10, 2024.

Kim, J., & Na, H. (2022). Interannual Variability of Yellowfin Tuna (*Thunnus albacares*) and Bigeye Tuna (*Thunnus obesus*) Catches in the Southwestern Tropical Indian Ocean and Its Relationship to Climate Variability. *Frontiers in Marine Science*, 9, 857405.

Kim, J., Na, H., Park, Y.-G., & Kim, Y. H. (2020). Potential predictability of skipjack tuna (*Katsuwonus pelamis*) catches in the Western Central Pacific. *Scientific Reports*, 10(1), 3193.

Kim, KY., Hamlington, B., & Na, H. (2015). Theoretical foundation of cyclostationary EOF analysis for geophysical and climatic variables: concepts and examples. *Earth-Science Reviews*, 150, 201–218.

Kim, KY., & North, G. R. (1997). EOFs of harmonizable cyclostationary processes. *Journal*

Of The Atmospheric Sciences, 54(19), 2416–2427.

Kim, K.Y., North, G. R., & Huang, J. (1996). EOFs of one-dimensional cyclostationary time series: Computations, examples, and stochastic modeling. *Journal of Atmospheric Sciences*, 53(7), 1007–1017.

Kim, S. T. (2012). A review of the Sea of Okhotsk ecosystem response to the climate with special emphasis on fish populations. *Ices Journal Of Marine Science*, 69(7), 1123–1133.

Kishi, S., Ohshima, K. I., Nishioka, J., Isshiki, N., Nihashi, S., & Riser, S. C. (2021). The prominent spring bloom and its relation to sea-ice melt in the Sea of Okhotsk, revealed by profiling floats. *Geophysical Research Letters*, 48(6), e2020GL091394.

Kosaka, S. (2000). Life history of Pacific saury *Cololabis saira* in the Northwest Pacific and consideration of resource fluctuation based on it. *Bull. Tohoku Nat. Fish. Res. Inst.*, 63, 1–95.

Kuroda, H., & Yokouchi, K. (2017). Interdecadal decrease in potential fishing areas for Pacific saury off the southeastern coast of Hokkaido, Japan. *Fisheries Oceanography*, 26(4), 439–454.

Liu, S., Liu, Y., Li, J., Cao, C., Tian, H., Li, W., . . . Li, Y. (2022). Effects of oceanographic environment on the distribution and migration of Pacific saury (*Cololabis saira*) during main fishing season. *Scientific Reports*, 12(1), 13585.

Megrey, B. A., Rose, K. A., Ito, S.-i., Hay, D. E., Werner, F. E., Yamanaka, Y., & Aita, M. N. (2007). North Pacific basin-scale differences in lower and higher trophic level marine ecosystem responses to climate impacts using a nutrient-phytoplankton–zooplankton model coupled to a fish bioenergetics model. *Ecological Modelling*, 202(1–2), 196–210.

- Miller, A. J., & Schneider, N. (2000). Interdecadal climate regime dynamics in the North Pacific Ocean: Theories, observations and ecosystem impacts. *Progress In Oceanography*, 47(2–4), 355–379.
- Miyamoto, H., Vijai, D., Kidokoro, H., Tadokoro, K., Watanabe, T., Fuji, T., & Suyama, S. (2020). Geographic variation in feeding of Pacific saury *Cololabis saira* in June and July in the North Pacific Ocean. *Fisheries Oceanography*, 29(6), 558–571.
- Mustapha, M. A., & Saitoh, S.-I. (2008). Observations of sea ice interannual variations and spring bloom occurrences at the Japanese scallop farming area in the Okhotsk Sea using satellite imageries. *Estuarine, Coastal and Shelf Science*, 77(4), 577–588.
- NPFC. (2021). *8th Meeting of the Small Scientific Committee on Pacific Saury Report NPFC-2021-SSC PS08-Final Report*. Retrieved from <https://www.npfc.int/meetings/8th-ssc-ps-meeting>
- NPFC. (2022). *10th Meeting of the Small Scientific Committee on Pacific Saury REPORT NPFC-SSC PS10-Report*. Retrieved from <https://www.npfc.int/meetings/8th-ssc-ps-meeting>
- NPFC. (2023a). *3rd intersessional meeting of the Small Scientific Committee on Pacific Saury NPFC-2023-SSC PS11-RP03*. Retrieved from <https://www.npfc.int/meetings/8th-ssc-ps-meeting>
- NPFC. (2023b). *11th Meeting of the Small Scientific Committee on Pacific Saury Report NPFC-2023-SSC PS11-Provisional Agenda*. Retrieved from <https://www.npfc.int/meetings/8th-ssc-ps-meeting>
- NPFC. (2023c). *12th Meeting of the Small Scientific Committee on Pacific Saury Report NPFC-2023-SSC PS12-IP06 The interannual to decadal relationship*

between total catch variability of Pacific saury (Cololabis saira) and basin-scale ocean environmental variability in the North Pacific. Retrieved from <https://www.npfc.int/meetings/8th-ssc-ps-meeting>

NPFC. (2023d). *12th Meeting of the Small Scientific Committee on Pacific Saury Report NPFC-2023-SSC PS12-WP06 Updates of stock assessment of Pacific saury (Cololabis saira) in the Western North Pacific Ocean through 2022.* Retrieved from <https://www.npfc.int/meetings/8th-ssc-ps-meeting>

NPFC. (2023e). *12th Meeting of the Small Scientific Committee on Pacific Saury Report NPFC-2023-SSC PS12-WP09 2023 updates on Pacific saury stock assessment in the North Pacific Ocean using Bayesian state-space production models (rev).* Retrieved from <https://www.npfc.int/meetings/8th-ssc-ps-meeting>

Oozeki, Y., Watanabe, Y., & Kitagawa, D. (2004). Environmental factors affecting larval growth of Pacific saury, *Cololabis saira*, in the northwestern Pacific Ocean. *Fisheries Oceanography*, *13*, 44–53.

Reynolds, R. W., Rayner, N. A., Smith, T. M., Stokes, D. C., & Wang, W. (2002). An improved in situ and satellite SST analysis for climate. *Journal Of Climate*, *15*(13), 1609–1625.

Saito, H., Tsuda, A., & Kasai, H. (2002). Nutrient and plankton dynamics in the Oyashio region of the western subarctic Pacific Ocean. *Deep Sea Research Part II: Topical Studies in Oceanography*, *49*(24–25), 5463–5486.

Suyama, S. (2002). Study on the age, growth, and maturation process of Pacific saury *Cololabis saira* (Brevoort) in the North Pacific. *Bull. Fish. Res. Agen.*, *5*, 68–113.

Tian, Y., Ueno, Y., Suda, M., & Akamine, T. (2002). Climate-ocean variability and the

response of Pacific saury (*Cololabis saira*) in the northwestern Pacific during the last half century. *Fisheries Science*, 68(sup1), 158–161.

Tian, Y., Akamine, T., & Suda, M. (2003). Variations in the abundance of Pacific saury (*Cololabis saira*) from the northwestern Pacific in relation to oceanic-climate changes. *Fisheries Research*, 60(2–3), 439–454.

Tian, Y., Ueno, Y., Suda, M., & Akamine, T. (2004). Decadal variability in the abundance of Pacific saury and its response to climatic/oceanic regime shifts in the northwestern subtropical Pacific during the last half century. *Journal Of Marine Systems*, 52(1–4), 235–257.

Tseng, C.-T., Su, N.-J., Sun, C.-L., Punt, A. E., Yeh, S.-Z., Liu, D.-C., & Su, W.-C. (2013). Spatial and temporal variability of the Pacific saury (*Cololabis saira*) distribution in the northwestern Pacific Ocean. *Ices Journal Of Marine Science*, 70(5), 991–999.

Tseng, C.-T., Sun, C.-L., Belkin, I. M., Yeh, S.-Z., Kuo, C.-L., & Liu, D.-C. (2014). Sea surface temperature fronts affect distribution of Pacific saury (*Cololabis saira*) in the Northwestern Pacific Ocean. *Deep Sea Research Part II: Topical Studies in Oceanography*, 107, 15–21.

Watanabe, K., Tanaka, E., Yamada, S., & Kitakado, T. (2006). Spatial and temporal migration modeling for stock of Pacific saury *Cololabis saira* (Brevoort), incorporating effect of sea surface temperature. *Fisheries Science*, 72, 1153–1165.

Watanabe, Y., Kurita, Y., Noto, M., Oozeki, Y., & Kitagawa, D. (2003). Growth and survival of Pacific saury *Cololabis saira* in the Kuroshio-Oyashio transitional waters. *Journal Of Oceanography*, 59, 403–414.

Watanabe, Y., & Lo, N. C. (1993). Larval Production and Mortality of Pacific Saury,

Cololabis saira, in the Northwestern Pacific Ocean¹. *Collected Reprints*, 2(3), 555.

White, K. J. (1992). The Durbin-Watson test for autocorrelation in nonlinear models. *The Review of Economics and Statistics*, 370–373.

Yasuda, I., & Watanabe, Y. (1994). On the relationship between the Oyashio front and saury fishing grounds in the north-western Pacific: a forecasting method for fishing ground locations. *Fisheries Oceanography*, 3(3), 172–181.

Yatsu, A., & Watanabe, K. (2017). Effects of environmental factors on long-term population fluctuations and a recent decline of stock abundance of Pacific saury in the waters of northern Japan. *Fisheries Management Department of the Tohoku National Fisheries Research Institute, FRA, Hachinohe*.

Author contributions

JK conducted the analysis, prepared the figures, and wrote the manuscript. JK designed the research and CR, LD, SN, MN, HS, YC, JH, VK, RK, RD, AZ, RM, and TK discussed the results. All authors contributed to the article and approved the submitted version.

Competing Interests

The authors declare no competing interests.

Acknowledgments

The authors appreciate the contributions of all NPFC members in collecting and verifying Pacific saury Catch and Effort data. The authors would also like to thank the reviewers, whose insightful comments and suggestions significantly improved the manuscript. Special thanks are due to Hyung-Ju Park, whose research on atmospheric-oceanic interaction and its impacts on marine ecology inspired the foundational concept of this study. The corresponding author extends heartfelt thanks to Prof. Kwang-Yul Kim, Professor of Climatology, Physical Oceanography, and Computational Science, whose development of Cyclostationary Empirical Orthogonal Function Analysis and dedication as an educator has been instrumental in providing guidance on the statistical interpretation for this study.

Data Availability Statement

The complete dataset used in this study, including supplementary information, is available in the published article. If additional details are needed, they can be obtained from the corresponding author upon justified request.

Figure set

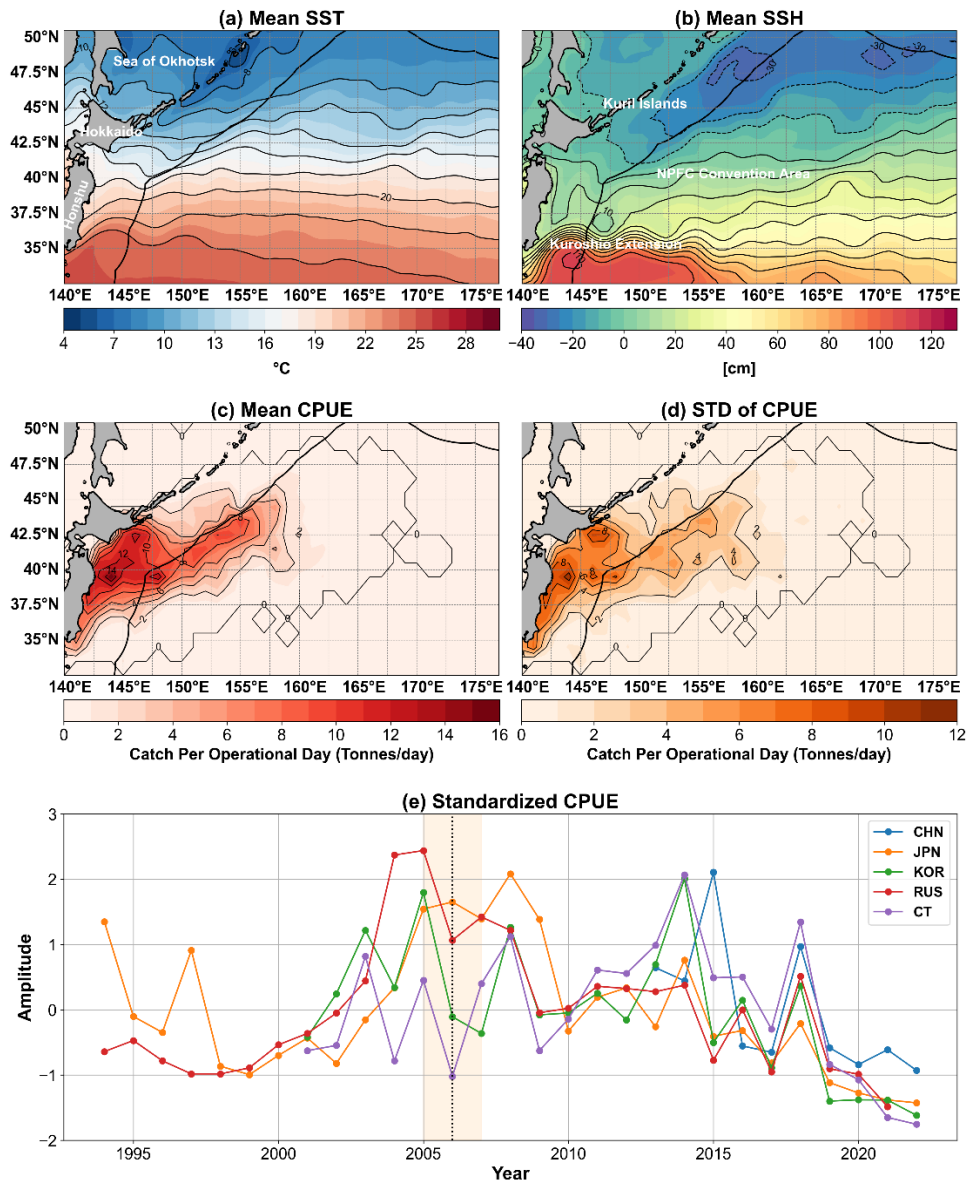


Figure 1. (a–b) The mean sea surface temperature (SST) and sea surface height (SSH). (c–d) The mean catch per operational day and its 2-year low-pass filtered standard deviations (STD) from August to December of each year during 2007–2022. The thick black lines indicate the North Pacific Fisheries Commission Convention Area. (e) Standardized catch per unit effort (CPUE) for each member of the North Pacific Fisheries Commission. The vertical black dotted line indicates the year 2006, and the orange shading highlights that year.

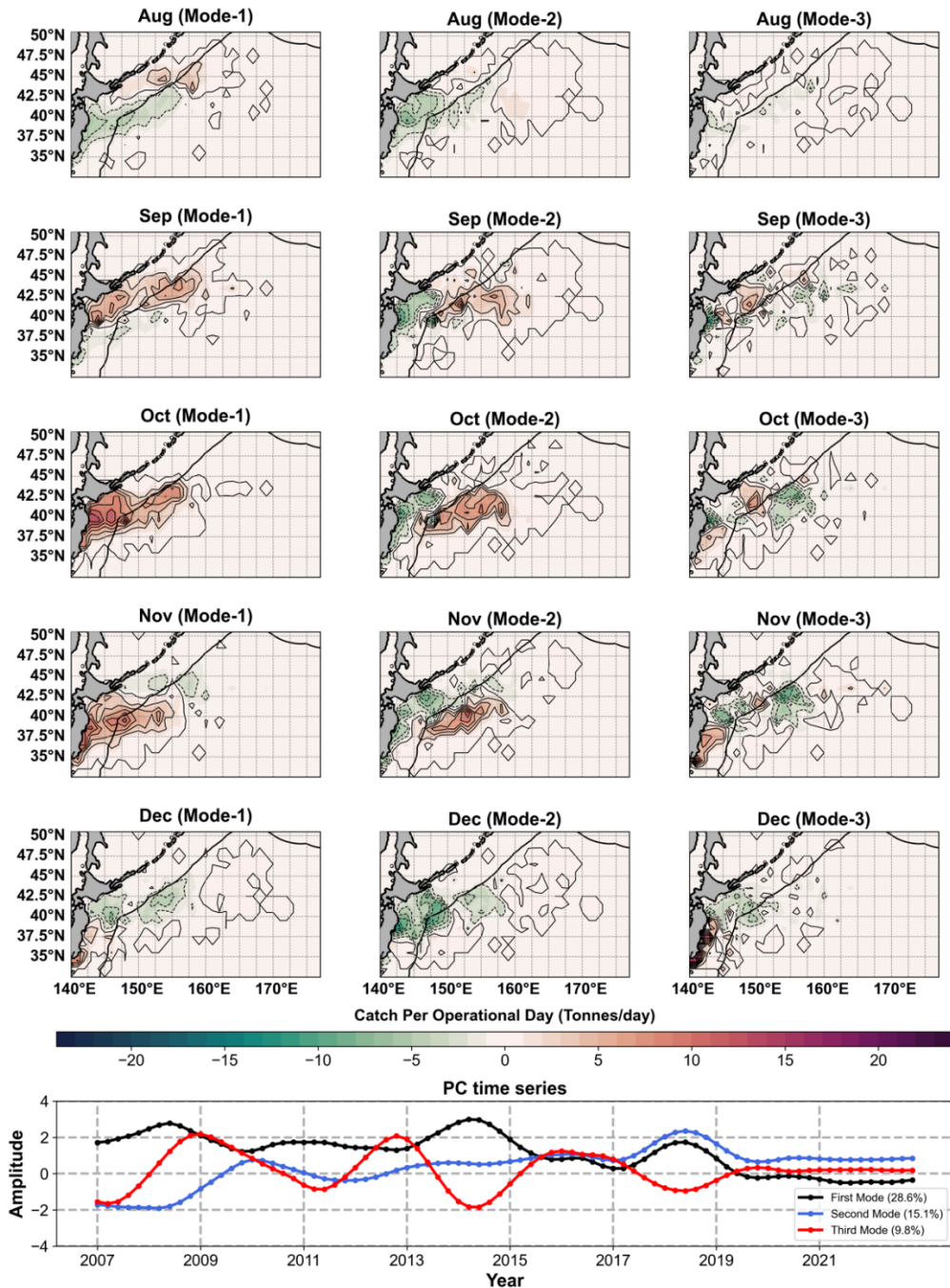


Figure 2. Cyclostationary loading vector (CSLV) and principal component (PC) time series for the leading three CSEOF modes of catch per operational day of Pacific saury: (left) the first mode, (middle) the second mode, and (right) the third mode from August to December of each year during 2007–2022. The number in parentheses in the legend of each mode represents its partial variance. The thick black lines indicate the North Pacific Fisheries Commission Convention Area.

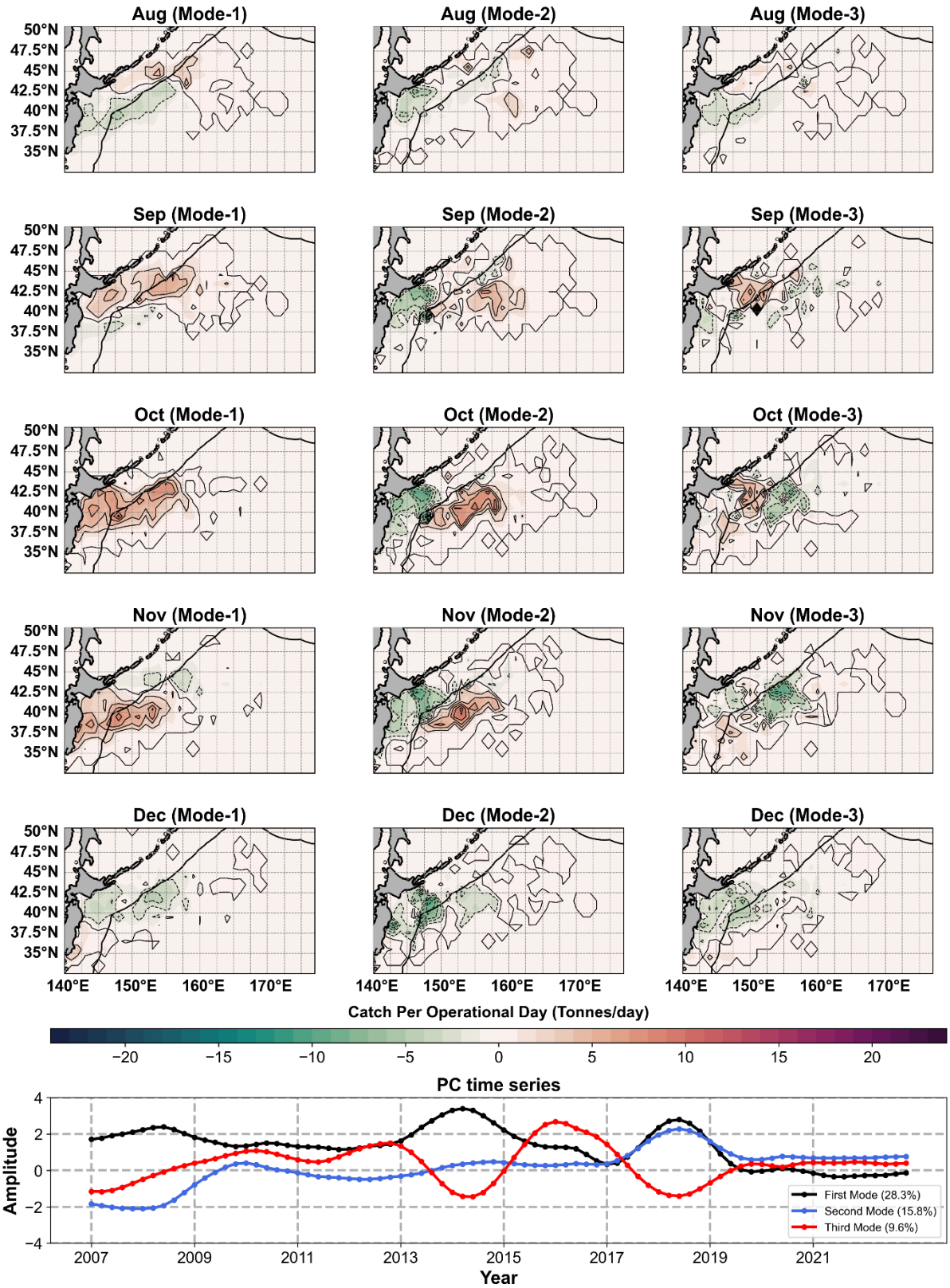


Figure 3. Same as Figure 2, but excluding JP1 data, which represents larger vessels.

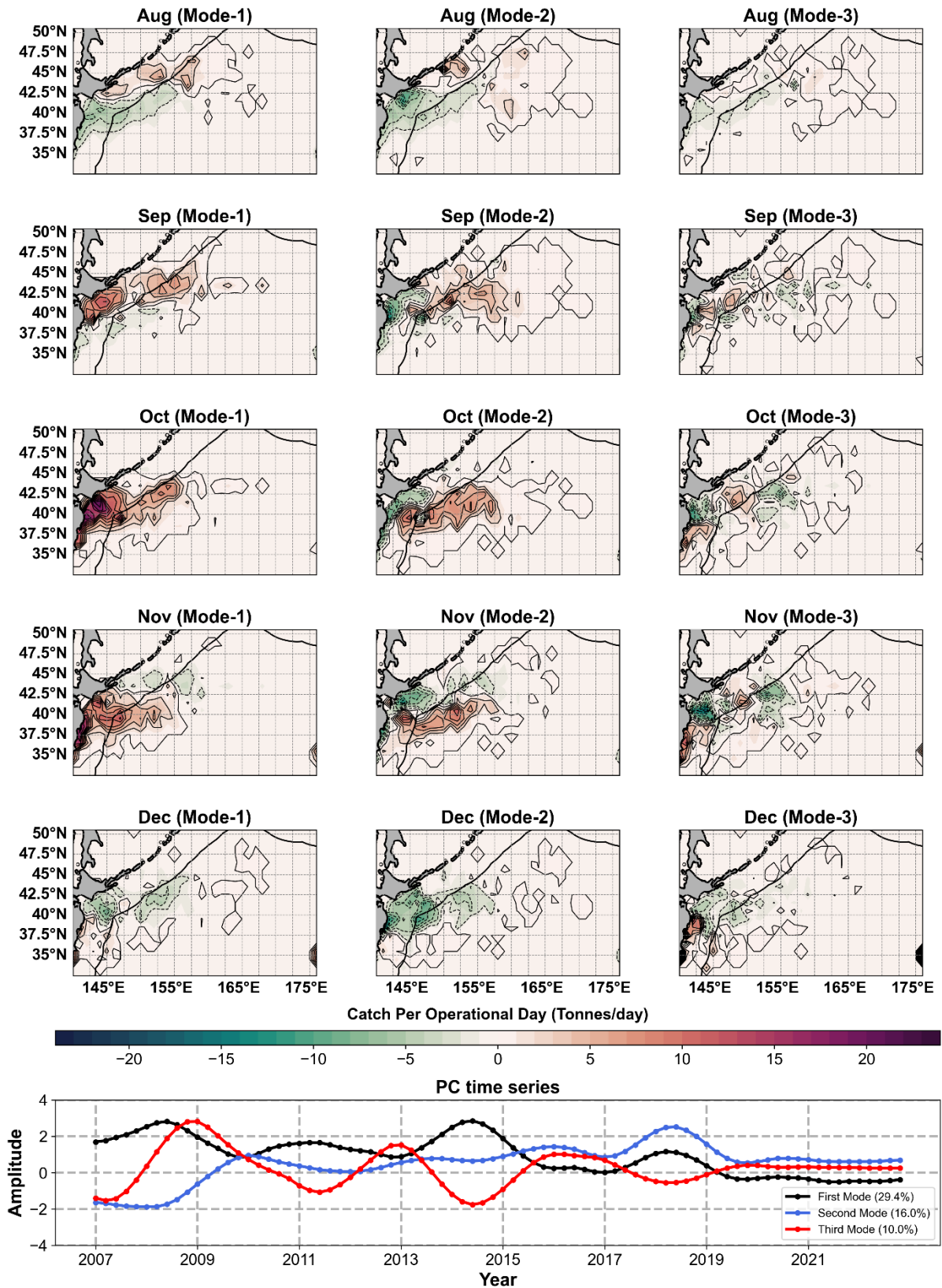


Figure 4. Same as Figure 3, but excluding JP2 data, which represents smaller vessels.

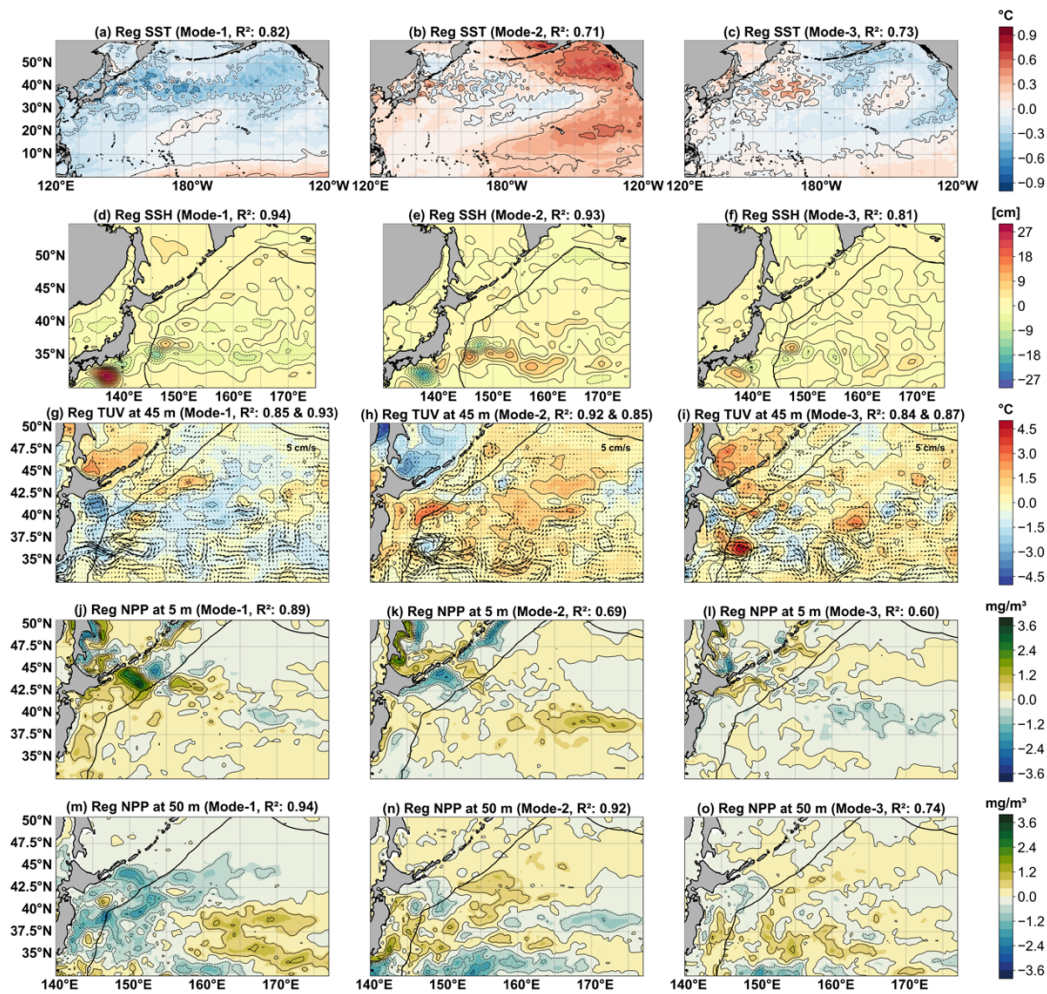


Figure 5. The yearly averaged regressed and reconstructed anomalies of the sea surface temperature (SST, contour interval: 0.25°C), sea surface height (SSH, contour interval: 3 cm), temperature with u and v components of current velocity (TUV, contour interval: 1°C), and net primary production (NPP, contour interval: 0.5 mg/m^3) in the North Pacific onto each mode of the Principal Component (PC) time series of catch per operational day of Pacific Saury in the Northwestern Pacific from August to December of each year during 2007–2022: (left) the first mode, (middle) the second mode, and (right) the third mode. The yearly averaged regressed and reconstructed anomalies of SSH, TUV, and NPP are shown only in the Northwestern Pacific. The R-squared value of each regression result is shown in each parenthesis. The thick black lines indicate the North Pacific Fisheries Commission Convention Area.

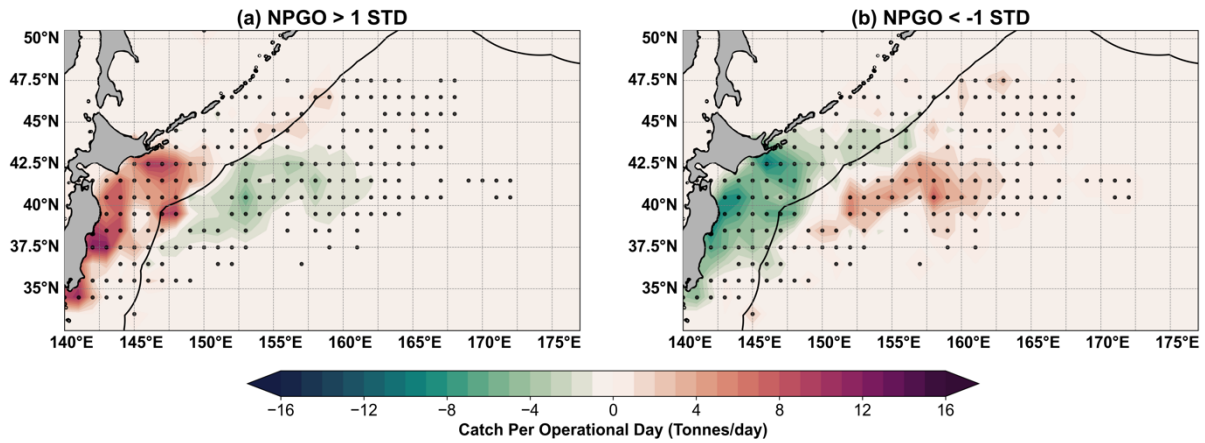


Figure 6. The spatial distributions of catch per operational day of Pacific saury in the Northwestern Pacific during the positive (left) and negative (right) phases of 2-year low-pass filtered North Pacific Gyre Oscillation (NPGO) exceeding or falling below one standard deviation during 2007–2022. Black dotted areas indicate statistically significant differences ($p < 0.05$) between positive and negative NPGO phases, determined by two-sample t-tests accounting for autocorrelation and adjusted for effective degrees of freedom, performed independently for each grid cell. The thick black lines delineate the North Pacific Fisheries Commission Convention Area.

Supplementary

Supplementary Table 1. Adjusted residual degrees of freedom (DOF) for each regression analysis involving ocean environmental variables—sea surface temperature (SST), sea surface height (SSH), temperature (T) and current velocity (UV) at 45 m depth, and net primary production (NPP) at 5 and 50 m depth—onto each mode of Pacific saury catch per unit effort (fishing days) variability, corrected for autocorrelation using the Durbin-Watson statistic and the Cochrane-Orcutt procedure.

	Residual DOF (Mode-1)	Residual DOF (Mode-2)	Residual DOF (Mode-3)
SST	49.16	42.7	44.69
SSH	47.02	44.4	46.24
T	34.67	32	34.42
UV	34.94	32.3	33.7
NPP (5m)	39.3	36.93	34.86
NPP (50m)	36.73	33.39	33.68